2010

Characterization of silver nanoparticles using flow-field flow fractionation interfaced to inductively coupled plasma mass spectrometry

A. R. Poda
US Army Engineer Research and Development Center, Aimee.R.Poda@usace.army.mil

A. J. Bednar
US Army Engineer Research and Development Center

A. Harmon
US Army Engineer Research and Development Center

M. Hull
NanoSafe, Inc

D. M. Mitrano
Colorado School of Mines

See next page for additional authors

Authors
A. R. Poda, A. J. Bednar, A. Harmon, M. Hull, D. M. Mitrano, J. F. Ranville, and J. Steevens

Journal of Chromatography A, xxx (2010) xxx–xxx

Contents lists available at ScienceDirect

Journal of Chromatography A

journal homepage: www.elsevier.com/locate/chroma

Characterization of silver nanoparticles using flow-field flow fractionation interfaced to inductively coupled plasma mass spectrometry

A.R. Poda[a,*], A.J. Bednar[a], A.J. Kennedy[a], A. Harmon[a], M. Hull[b,c], D.M. Mitrano[d], J.F. Ranville[d], J. Steevens[a]

[a] US Army Engineer Research and Development Center, Environmental Laboratory, 3909 Halls Ferry Rd., Vicksburg, MS 39180, USA
[b] NanoSafe, Inc., 2200 Kraft Drive, Suite 1200 I, Blacksburg, VA 24060, USA
[c] Department of Civil and Environmental Engineering, Institute for Critical Technology and Applied Science (ICTAS), International Center for the Environmental Implications of Nanotechnology (iCEINT), Virginia Tech, Blacksburg, VA, USA
[d] Department of Chemistry and Geochemistry, Colorado School of Mines, Golden, CO, USA

ARTICLE INFO

Article history:
Available online xxx

Keywords:
Nanoparticle characterization
FFF
ICP-MS
Comparison techniques
Natural matrices

ABSTRACT

The ability to detect and identify the physiochemical form of contaminants in the environment is important for degradation, fate and transport, and toxicity studies. This is particularly true of nanomaterials that exist as discrete particles rather than dissolved or sorbed contaminant molecules in the environment. Nanoparticles will tend to agglomerate or dissolve, based on solution chemistry, which will drastically affect their environmental properties. The current study investigates the use of field flow fractionation (FFF) interfaced to inductively coupled plasma-mass spectrometry (ICP-MS) as a sensitive and selective method for detection and characterization of silver nanoparticles. Transmission electron microscopy (TEM) is used to verify the morphology and primary particle size and size distribution of precisely engineered silver nanoparticles. Subsequently, the hydrodynamic size measurements by FFF are compared to dynamic light scattering (DLS) to verify the accuracy of the size determination. Additionally, the sensitivity of the ICP-MS detector is demonstrated by fractionation of μg/L concentrations of mixed silver nanoparticle standards. The technique has been applied to nanoparticle suspensions prior to use in toxicity studies, and post-exposure biological tissue analysis. Silver nanoparticles extracted from tissues of the sediment-dwelling, freshwater oligochaete *Lumbriculus variegatus* increased in size from approximately 31–46 nm, indicating a significant change in the nanoparticle characteristics during exposure.

Published by Elsevier B.V.

1. Introduction

Nanotechnology is a rapidly developing field, attracting significant investment from government, industry, and academia [1]. Material applications have already yielded a variety of commercially available products including cosmetics, antimicrobials, suntan lotions, paints, stain-resistant clothing and remediation products [2]. This increase in nanomaterial production poses concerns for environmental safety with the potential release of nanomaterials into the environment. Understanding the environmental behavior of nanomaterials in different environmental matrices is highly challenging. Due to their small size, nanomaterials, exhibit physiochemical properties that differ from those of other bulk materials; hence their environmental fate and effects are largely unknown.

The bioavailability and potential toxicity of these materials depend on their dispersion, transport and fate through the different media encountered in the environment [3]. Nanomaterial aggregation, deposition, and dissolution behaviors factor into transport potentials and the subsequent environmental fate and ecotoxicological impacts of these materials. To quantify the stability of nanoparticles in the environment, the stability of their suspensions and their tendency to aggregate and interact with other particles must first be determined [4]. Recent reviews have touched upon the challenges associated with characterizing nanomaterials in environmental settings stressing the importance of not only the material specific properties (size, shape, and chemical composition), but also the role that surface coatings play in determining the reactivity, surface attachment and agglomeration properties of nanomaterials [5–7]. Therefore, no definitive conclusions on nanoparticle fate can be made without sufficient characterization and a quantitative understanding of nanoparticle properties in relevant environmental matrices.

A range of analytical techniques are available for providing information on concentration and particle size distributions,

* Corresponding author. Tel.: +1 601 634 4003; fax: +1 601 634 2742.
E-mail address: Aimee.R.Poda@usace.army.mil (A.R. Poda).

0021-9673/$ – see front matter. Published by Elsevier B.V.
doi:10.1016/j.chroma.2010.12.076

including microscopy approaches [8,9], chromatography [10,11], centrifugation [12], laser scattering [13] filtration [14–16], spectroscopic [17,18] and related techniques. Generally, difficulties arise due to a lack of analytical tools capable of characterizing and quantifying particles at environmentally relevant concentrations (low ppb) or in complex environmental matrices that may induce heterodisperse particle size distributions [19]. To date there have been few measurements of manufactured nanoparticles in natural waters or soils because of the extreme difficulty in detecting those at environmentally relevant concentrations [20,21] while avoiding the potential interference of natural nanoparticles frequently present in environmental samples [22].

It has been reported that the average size and size distribution of nanoparticles can significantly vary when comparing results from different techniques [23]. Each technique is not without limitations and, therefore inaccurate predictions of material properties and structure can result. Correct size measurements are difficult, depending on the tool applied and the media in which the particles are dispersed. Electron microscopy (EM) and dynamic light scattering (DLS) are the most commonly used techniques. Both have advantages and disadvantages [24]. EM gives the most direct information on the size distribution and shapes of the primary particles, however there is concern about artifacts introduced by the sample preparation step attributed to the lack of a representative sample. In addition, organic coatings that are not visible in the electron microscope (due to light elements, such as carbon) can lead to discrepancies in sizing, especially when compared to sizing tools that measure the hydrodynamic diameter of particles. Dynamic light scattering (DLS) measures the particle hydrodynamic diameter, but limitations include: poor sensitivity at dilute concentrations, non-selective material detection, inability to distinguish mixtures or complex matrices and little capability to count particles to resolve the dominant size in multi-modal particle or aggregate size distributions. With DLS, the presence of a relatively small number of large aggregates will skew the effective diameter of a distribution of predominantly smaller particles toward a larger particle size distribution.

For studies of nanoparticles, field flow fractionation (FFF) has been advocated, in particular, a variation called flow field flow fractionation (FFFF) [25,26]. FFF is a family of separation techniques designed to separate particles based on diffusion coefficient, and when coupled to an elemental specific detector, such as ICP-MS, particle composition as a function of hydrodynamic size can be determined. This paper describes the development and application of an FFF–ICP-MS method for the characterization of silver nanoparticle mixtures. It has been applied to two types of particles known to have stable aqueous suspensions. The primary advantages over DLS and EM are demonstrated with element/particle specific detection and the ability to size particle mixtures. Furthermore, the addition of the sensitive and selective ICP-MS detector allows for determination of silver nanoparticles at environmentally relevant concentrations (low ppb). Furthermore, the technique is applied to biological media to characterize silver nanoparticles before and after exposure to the freshwater oligochaete, *Lumbriculus variegatus*.

2. Materials and methods

2.1. Nanosilver particles

Two sources of silver nanoparticles were investigated in the current study. Aqueous NanoXact silver nanoparticle suspensions ranging in size from 10 to 80 nm were supplied by Nanocomposix (San Diego, CA). These particles were generally monodisperse in size and were acquired in 10 nm increments ranging from 10 to 80 nm as nominal 20 mg/L suspensions. The 10 nm silver particles were stabilized in 2 mM citrate buffer solutions, while the particles ranging in size from 20 to 80 nm were stabilized in 2 mM phosphate buffer solutions as described by the manufacturer. Secondly, a polyvinylpyrrolidone (PVP)-coated nanosilver, produced by Luna Innovations (Blacksburg, VA, USA) by reduction of $AgNO_3$ in ethylene glycol (solvent and reducing agent) with PVP added for stabilization, was also utilized. The raw reaction product was dialyzed against water to remove ethylene glycol, unbound PVP and Ag^+ that may have been present.

2.2. Transmission electron microscopy

Transmission electron micrographs (TEM) of the dried silver NanoXact silver particles were obtained by subsampling particle suspensions (10–20 μL) using a Zeiss 10CA TEM (Zeiss, Oberkochen, Germany) operating at 60 kV and equipped with an AMT Advantage GR/HR-B CCD Camera digital imaging system. The longest dimension of all distinct particles (≥202 per material analyzed) that were observed in each of 10 images was manually analyzed using Image-Pro® Plus software Version 7.0 (Media Cybernetics Inc., Bethesda, MD, USA). The scale bar from the TEM images was used to calibrate the software.

2.3. Dynamic light scattering

Dynamic light scattering hydrodynamic size of the silver NanoXact particles was obtained using a 90 Plus/BI-MAS (Brookhaven Instruments, Holtsville, NY, USA) instrument applying a 660 nm laser oriented at 90° relative to the sample. The software was optimized to report summary statistics based upon the intensity of light scattered. Two mL sample volumes from each nanosilver dispersion (10 mg/L nominal) were loaded into glass cuvettes (supplied by manufacturer) and summary statistics were obtained using triplicate 3 min analyses (total analysis time = 9 min). Instrument performance was verified using a polymer reference standard known to be 92 ± 3.7 nm (NIST traceable diameter, Duke Scientific, 3090A, Palo Alto, CA, USA).

2.4. FFF–ICP-MS

The instrument used for all studies was an F-1000 symmetrical flow field flow fractionation (FFF) system from Postnova Analytics (Salt Lake City, UT), interfaced to a PerkinElmer Elan DRC II ICP-MS using a MiraMist pneumatic nebulizer. An Agilent 1100 variable wavelength detector was placed in-line between the FFF and ICP-MS systems to collect UV absorption data, primarily for detection of polystyrene bead size standards. UV absorbance data was not collected for the dilute nanosilver particles measured due to the limited absorbance of the silver nanoparticles at the low concentrations (μg/L) studied. The FFF system was equipped with a 10kDa regenerated cellulose membrane. The mobile phase consisted of a 0.025% sodium azide and 0.025% FL-70 surfactant dissolved in deionized water with a resistivity of 18.3 MΩ cm. Separation of the particles under investigation was achieved using a channel flow of 1.0 mL/min and a cross flow of 0.75 mL/min. The channel flow conditions allow direct connection of the FFF effluent to the ICP-MS nebulizer without a flow splitter. Additional details of the FFF separation conditions are listed in Table 1.

The ICP-MS was operated in standard mode due to the lack of interferences on the 2 isotopes of silver (^{107}Ag and ^{109}Ag). The plasma was operated at 1250 W and the nebulizer flow at 0.8 mL/min. Both silver isotopes were monitored for detection and confirmation, each had an integration dwell time of 500 ms, resulting in a data point being collected at a rate of approximately 1 per second. The number of readings per replicate was chosen such that

Please cite this article in press as: A.R. Poda, et al., J. Chromatogr. A (2011), doi:10.1016/j.chroma.2010.12.076

Table 1
Analytical instrumentation parameters used for separation and characterization of silver nanoparticles by FFF–ICP-MS.

FFF system	Postnova F-1000 Symmetrical
Membrane	10 kDa regenerated cellulose
Channel and cross flow	1.0 and 0.75 mL/min, respectively
Injection volume	50 μL
Load time	15 s
Relaxation time	3.2 min
Approximate fractogram time (100 nm elution)	25 min
UV absorbance detector	Agilent 1100 VWD
Wavelength monitored	254 nm
Integration time	0.4 s
ICP-MS	PerkinElmer Elan DRC II
Plasma power	1250 W
Nebulizer, spray chamber, and flow	MiraMist, Double Pass Scott, 0.8 mL/min
Masses monitored	^{107}Ag, ^{109}Ag
Dwell time per AMU	500 ms
Readings per replicate	1600

data were collected for the entire length of the fractogram, usually for about 25 min. Table 1 also lists the operating conditions for the variable wavelength detector and ICP-MS.

2.5. Calibration

The theory behind FFF separation and sizing is well developed [27–29]. One of the advantages of flow FFF for particle size determination is that elution time under identical processing conditions (cross-flow and channel flow settings, carrier solution, etc.) is solely related to particle size, and follows a linear correlation [30]. In this paper, flow FFF was used to determine mean particle size as a function of fractogram elution time using NIST-traceable polystyrene bead size standards obtained from Postnova Analytics (Art. Nr. z-PS-POS-000-0 (02:05:1)). A three bead mixture (20, 50, and 100 nm) was created by dilution of the single-size stock standards (1% solids in 15 ml) in deionized water to a final concentration of approximately 80 mg/L for each particle size.

The fractograms of the polystyrene bead mixture shown in Fig. 1 illustrate this size-distribution of particles is well-resolved. Data from three replicate injections approximately 24 h apart was collected for Fig. 1 showing excellent reproducibility. The small peak at about 275 s is the "void peak" representing the material not retained by the field. The elution time at maximum absorbance was related to the mean particle size of the polystyrene standards. Retention time from the UV absorbance fractogram of the polystyrene standards was then used to establish a linear response function of size vs. elution time, as shown in Fig. 1 inset. Typical correlation coefficients from the three point calibration are greater than 0.9999. This linear response function was used in conjunction with the ICP-MS data to determine the mean particle size for the nanosilver examined in this study.

2.6. Quantitative analysis

Quantitative analyte recovery experiments designed to determine the amount of nanoparticle loss to the FFF separation system and ICP-MS sample introduction system were performed. This analysis addresses concerns over nanosilver analysis, namely loss of NPs due to adhesion to physical surfaces of the membrane, tubing and spray chamber. Recoveries of the three silver nanoparticle sizes tested (10, 40, and 70 nm) with the cross flow field on, cross flow field off, and bypassing the FFF entirely yielded recoveries of 88–98% based on integrated peak areas, which is deemed excellent recovery for any traditional metals analysis [31]. While some loss of particles can be expected due to interactions with the FFF membrane, minimal loss occurs to the ICP-MS sample introduction system, although only about 5–10% of the sample is actually aspirated into the plasma, due to known nebulizer efficiencies.

2.7. Biological exposure

A freshwater sediment (Browns Lake, Vicksburg, MS, USA) was nominally spiked at 100 mg Ag/kg (measured = 70 mg/kg) with the PVP-coated silver nanoparticle (described above) and aged for two weeks. Following the aging period, the freshwater oligochaete *L. variegatus* was exposed to the sediment for 28 days following standard method guidance [32]. Organisms were removed from the sediment, depurated as specified by method guidance [32] composited from each experimental replicate, and frozen. Prior to FFF analysis, 1.0 g of frozen tissue was added to 10 mL of deionized water and sonicated for 1 h and then centrifuged to remove biological debris. The supernatant was then analyzed by FFF–ICP-MS.

2.8. Statistical analysis

Data normality (Kolmogorov–Smirnov's test), homogeneity (Levene's test), and one-way ANOVA and Tukey's test were determined at the $\alpha = 0.05$ level. The results from the different particle sizing techniques were compared by Pearson product moment correlation. All analyses were performed using SigmaStat Software (SSPS, Chicago, IL, USA).

3. Results and discussion

3.1. Transmission electron microscopy

The TEM images shown in Fig. 2 demonstrate the spherical shape and narrow particle size distribution of the NanoXact silver nanoparticles. Manual size analysis of the individual particles over a range of TEM magnifications is listed in Table 2. The average primary particle size is very close to the nominal size reported by the manufacturer. There is some indication that the 60 nm size particles are slightly larger than the reported (67 nm by TEM vs. nominal 60 nm), yet overall agreement within 1–5 nm is observed (except the 60 nm) with similar size standard deviations for each particle size.

3.2. Dynamic light scattering

Hydrodynamic effective diameters of the particles measured by DLS are listed in Table 2. As expected, the hydrodynamic diameter is slightly larger than the primary particle size, indicative of a surface layer of the stabilizing agent and/or the hydration sphere. The DLS effective diameter ranges reported above may be indicative of some occurrence of particle aggregation in aqueous suspension. The autocorrelation function indicated acceptable data capture for all analyzed particles, the baseline index ranged from 6.0 to 9.5 (exceptions: NC10 = 0; NC20 = 1.3) and the data retention ranged from 93% to 100%. The count rate (kcps) ranged from 136 to 490, although substantially lower (16) for nominal 10 nm particles. It is noteworthy that the comparisons between TEM primary particle size, FFF and DLS are very close in this study partially due to the tight particle size distribution of the NanoXact materials. In cases where much more polydisperse primary particle (or aggregate) sizes are found in suspension [35], larger discrepancies between FFF and DLS outputs are likely to be observed due to differences in how particle sizes are determined and how summary parameters are weighted

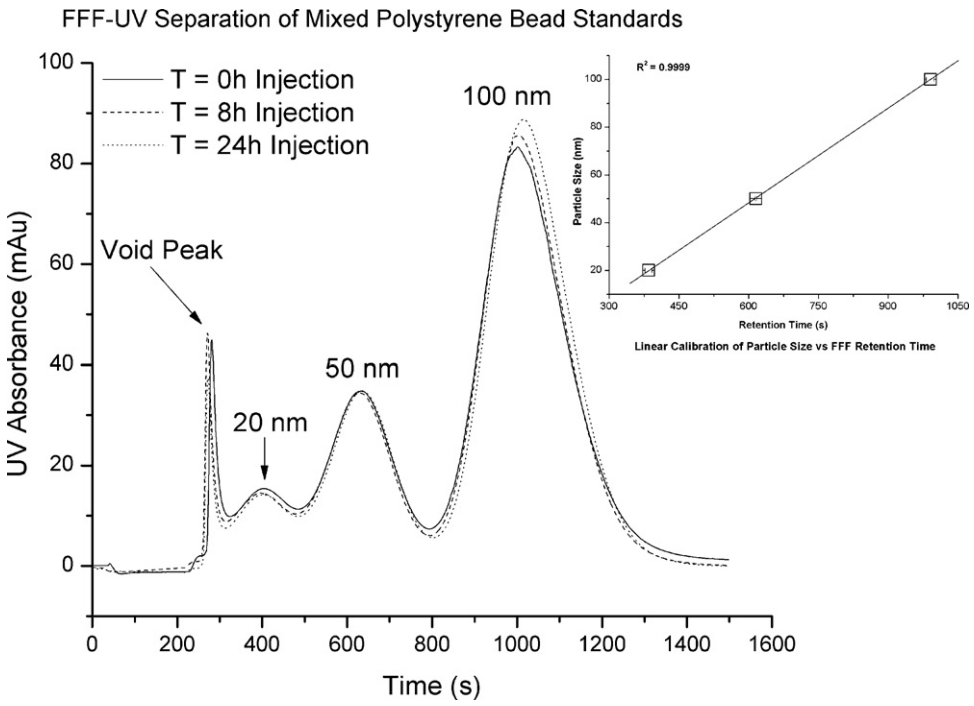

Fig. 1. Overlay of triplicate FFF-UV fractograms of polystyrene bead calibration standards. FFF separation conditions were 1.0 mL/min channel flow and 0.75 mL/min cross flow. UV absorbance detection is at 254 nm wavelength. Inset: Linear regression calibration function using 20, 50, and 100 nm polystyrene bead standards. Error bars represent standard deviation of the triplicate retention times obtained from UV absorbance data at maximum absorbance.

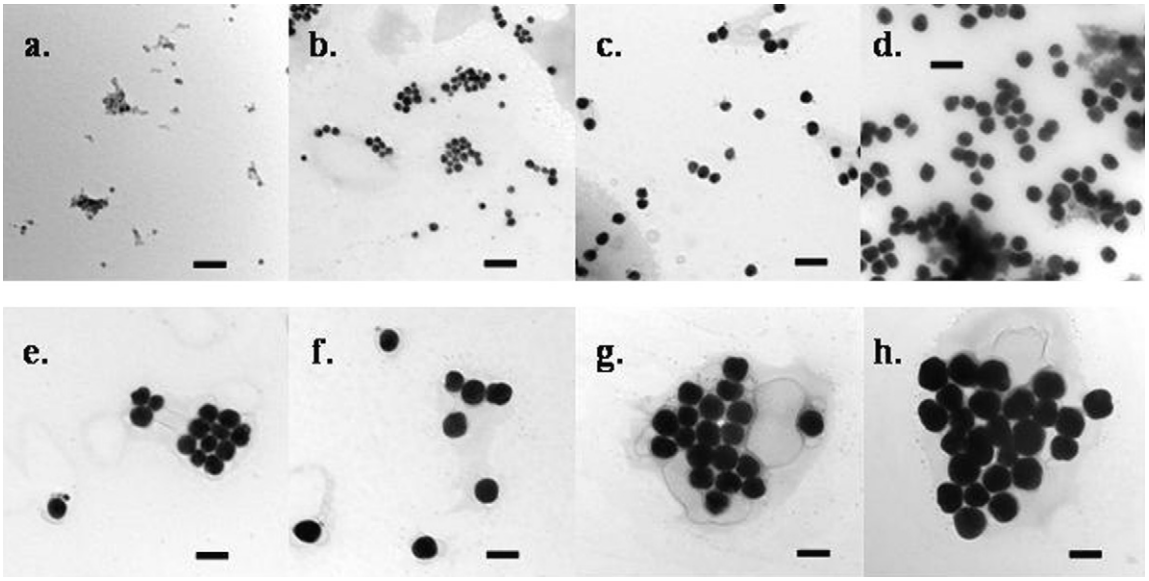

Fig. 2. TEM panels showing, in order from a to h, 10, 20, 30, 40, 50, 60, 70, and 80 nm particles. All particles were imaged at 125k magnification. Scale bars denote 100 nm.

Table 2
Size determinations by three independent analytical techniques for the NanoXact silver nanoparticles. Ranges are provided in parentheses.

	Nominal							
	10 nm	20 nm	30 nm	40 nm	50 nm	60 nm	70 nm	80 nm
Mean TEM ± Std. dev. (size range)	9 ± 1 (2–20)	20 ± 1 (5–33)	32 ± 4 (5–48)	42 ± 4 (16–60)	55 ± 5 (35–74)	67 ± 4 (38–88)	72 ± 3 (16–89)	84 ± 5 (48–112)
DLS effective diameter (size range)	22 (11–84)	29 (13–90)	41 (15–124)	51 (35–113)	54 (14–121)	67 (32–133)	74 (64–104)	86 (58–142)
FFF–ICP-MS mean hydro-dynamic diameter	26	31	40	52	61	75	76	86

Please cite this article in press as: A.R. Poda, et al., J. Chromatogr. A (2011), doi:10.1016/j.chroma.2010.12.076

(e.g., DLS intensity analysis is weighted toward the larger particles in the dispersion).

3.3. FFF separation and sizing

Size fractionation of the NanoXact particles by serial filtration was examined prior to the FFF separation method development. Serial filtration is generally an appealing approach because of its low cost and ease of use. However filtration size resolution is limited by the available filter pore sizes. Of more concern, however, is that separation results were highly variable and dependant not only on the filter pore size but also on the composition of the filtration membrane [33]. Therefore, the need to develop the FFF separation method was critical.

The overlays shown in Fig. 3 are FF fractograms of the individual NanoXact particles obtained under the standardized processing conditions (Table 1) by FFF–ICP-MS. The concentration of silver in each Injection was 200 μg/L. The size data obtained from the FFF analysis listed in Table 2 agrees well with the DLS size results. In both cases the size measurements are slightly larger than the TEM results and are reflective of measurement techniques specific to the measurement of the hydrodynamic diameter rather than the primary particle. Under the flow conditions outlined in Table 1, baseline resolution of nanomaterials that vary in size by 10 nm was not obtained. However, sufficient resolution was achieved for sizing the subject particles based on maximum peak intensity. The nominal 60 and 70 nm particles graphed in Fig. 3 are in agreement with the DLS results with sizes reported in Table 2 that are nearly the same. This is clearly demonstrated as the fractograms nearly overlap, indicating the similar size of these two nanoparticles.

To demonstrate the separation and detection potential of the FFF–ICP-MS method more clearly, Fig. 4 shows a mixture of the nominal 10, 40, and 70 nm silver nanoparticles, each particle present at a total silver concentration of 67 μg/L. The particles produced clearly defined peaks under these separation conditions, although baseline resolution was not achieved. The noise of the

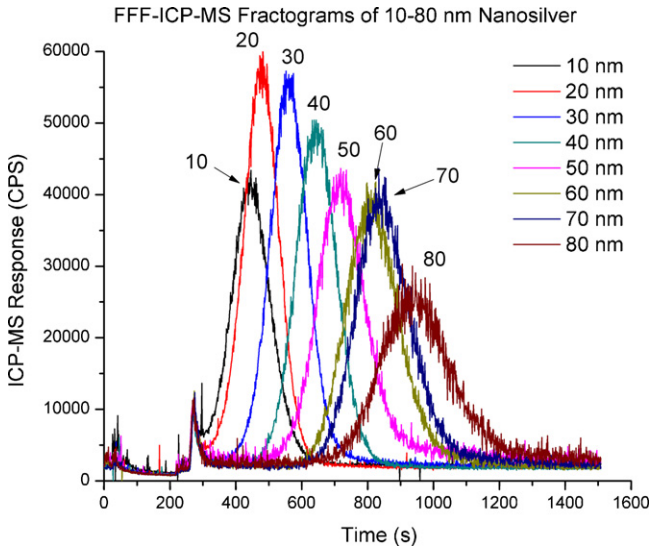

Fig. 3. Individual FFF–ICP-MS fractograms overlain of NanoXact silver nanoparticles. Each peak represents 200 μg/L total silver as nanosilver particles. FFF separation conditions were 1.0 mL/min channel flow and 0.75 mL/min cross flow with ICP-MS detection using ^{107}Ag.

signals appears to increase with the nanoparticle size. It is hypothesized that the larger nanoparticles may result in more 'spikes' in the ICP-MS signal due to the delivery of larger amounts of silver into the plasma/detector system per particle unit. This phenomena is described in the use of ICP-MS as a 'single particle counter' currently being developed by several research groups [34].

Also shown in Fig. 5 is a 1:5 dilution of the 67 μg/L sample, which yields a total silver concentration for each particle of approximately 13.4 μg/L. Although the fractogram peaks are quite small, they are still clearly defined at this concentration level. To further test the sensitivity of the ICP-MS detector, the inset in Fig. 5 shows a 1:10

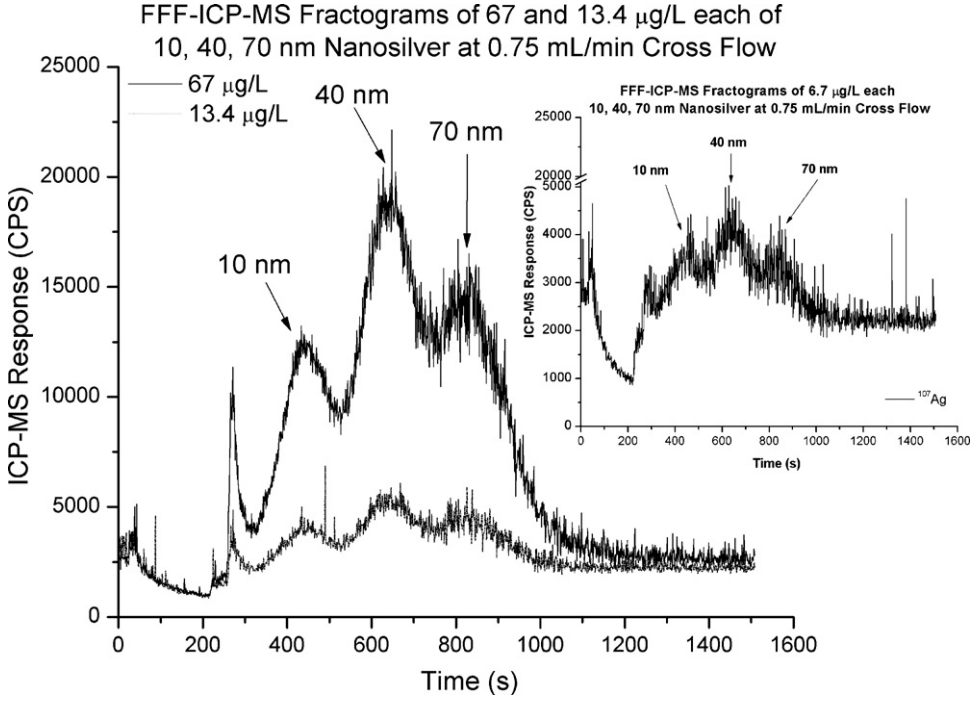

Fig. 4. FFF–ICP-MS fractograms of a mixture of 10, 40, and 70 nm silver particles at 67 and 13.4 μg/L each. FFF separation conditions were 1.0 mL/min channel flow and 0.75 mL/min cross flow with ICP-MS detection using ^{107}Ag. Inset: FFF–ICP-MS fractogram of a mixture of 10, 40, and 70 nm silver particles at 6.7 μg/L each. FFF separation conditions were 1.0 mL/min channel flow and 0.75 mL/min cross flow with ICP-MS detection using ^{107}Ag.

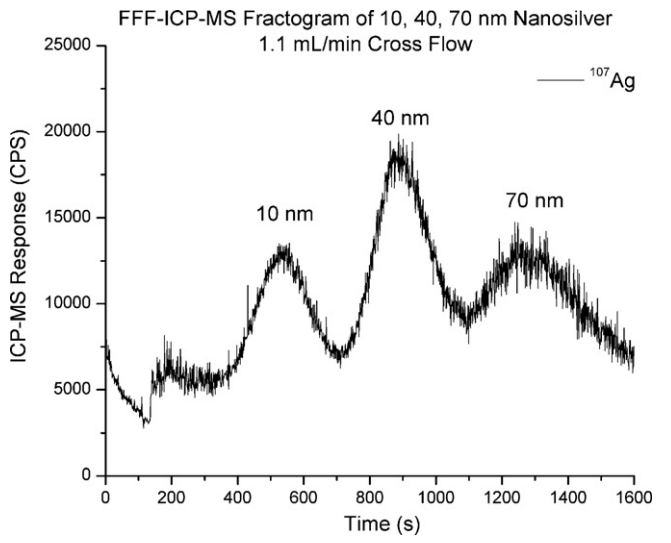

Fig. 5. FFF–ICP-MS fractogram of a mixture of 10, 40, and 70 nm silver particles at 67 μg/L each. FFF separation conditions were 1.0 mL/min channel flow and 1.1 mL/min cross flow with ICP-MS detection using ^{107}Ag.

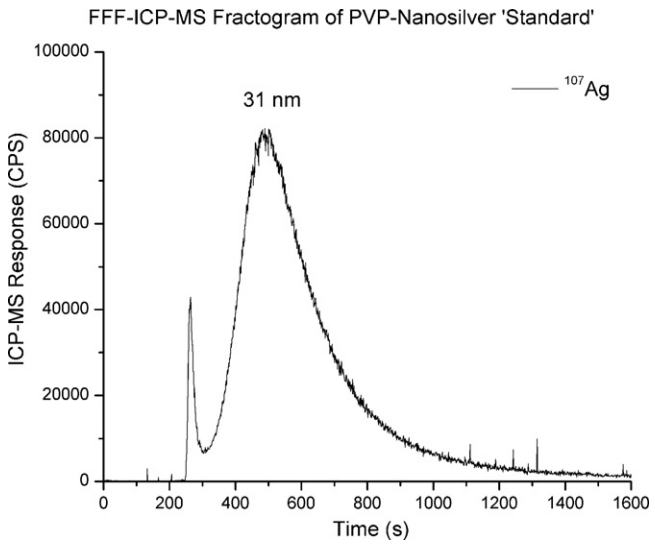

Fig. 6. FFF–ICP-MS fractogram of the stock PVP-coated silver nanoparticle in deionized water. FFF separation conditions were 1.0 mL/min channel flow and 0.75 mL/min cross flow with ICP-MS detection using ^{107}Ag.

dilution of the 67 μg/L mixture, yielding a total silver concentration of 6.7 μg/L for each particle size. At this concentration, the ICP-MS signal is quite noisy, yet three peaks are still sufficiently defined in the fractogram to characterize the particle size, which suggests the method is applicable to detection and characterization of silver nanoparticles at concentrations less than 10 μg/L.

Improved separation of the 10, 40, and 70 nm particle mixture would be ideal, therefore, as shown in Fig. 5, increasing the cross flow to 1.1 mL/min, further increases separation with minimal reduction in sensitivity and minor peak broadening. Under these flow conditions, the separation is improved with similar sensitivity, and only a minimal sacrifice in analytical time.

3.4. Comparison of size measurements

Pearson correlations of all of the size measurement techniques (manufacturer nominal size, TEM, DLS, FFF) resulted in very strong and significant correlations ($r > 0.99$; $p < 0.001$). Comparisons of the slopes of linear regressions of the measurement techniques (Table 3) indicated that the measures of hydrodynamic diameter (DLS and FFF) had the best correlation (slope = 1.000), followed by nominal size vs. TEM primary particle size (slope = 1.075) and nominal size vs. FFF (slope = 0.904). The smallest slope (0.830) was observed for TEM primary particle size vs. DLS, which is only partially due to the relatively larger than expected effective diameter of the 10 nm particle (Table 2). This may be primarily explained by the DLS measuring of the hydrodynamic diameter of the particles, which is by definition larger than the primary particle size (note that TEM vs. FFF also results in a relatively small slope for the same reasons). This is further supported by *y*-intercepts being closest to zero for more similar measurement techniques, i.e., the measurement techniques that elucidate primary particle size (manufacturer nominal vs. TEM primary particle size) and hydrodynamic diameter (DLS vs. FFF) had intercepts approximating zero; −0.75 and 2.891, respectively.

Table 3
Results of linear regression analysis of the different particle sizing techniques employed in this investigation.

Methods compared	R^2	*y*-Intercept	Slope
Nominal vs. TEM	0.995	−0.75	+1.075
Nominal vs. DLS	0.992	+12.607	+0.898
Nominal vs. FFF	0.985	+15.214	+0.904
TEM vs. DLS	0.986	+13.458	+0.830
TEM vs. FFF	0.992	+15.79	+0.842
DLS vs. FFF	0.979	+2.891	+1.000

3.5. Application to biological exposures

The above described FFF–ICP-MS technique was subsequently applied to characterization of nanoparticles after exposure to a biological receptor. Specifically, the freshwater oligochaete *Lumbriculus variegates*, was exposed to PVP-coated nanosilver spiked sediment as described above. In order to determine the effect of environmental exposure on the nanoparticle physiochemical form, the stock nanoparticles were first analyzed by FFF–ICP-MS, as shown in Fig. 6. Comparison to the polystyrene size calibration indicates the PVP-silver particles produce a stable dispersion and have an average hydrodynamic size of about 31 nm.

After the 28-day biological exposure, the tissues were extracted with deionized water using sonication, with the resultant supernatant analyzed by FFF–ICP-MS, as shown in Fig. 7. The silver nanoparticles extracted from the tissue have an average hydrodynamic size of approximately 46 nm, compared to the original 31 nm. This size increase may indicate coating of the particles with proteins or other biological molecules. However, because no data are available on the coating from this analysis, it is possible that biological mechanisms, or abiotic reactions in the soil exposure medium, have removed the stabilizing PVP coating, resulting in aggregation of the resulting destabilized silver particles. Additional work is underway to discern the exact mechanism, yet these preliminary results demonstrate that exposure of nanoparticles to environmental media (sediment or biological) can change the particle physiochemical form and FFF–ICP-MS can be successfully used to characterize nanomaterials extracted from such complex media. Unfortunately, recovery of particle vs. total silver loading cannot be determined for the biological sample as the particles were extracted using a deionized water and sonication method, which has an unknown extraction efficiency. Total silver analysis is routinely accomplished with aggressive acid digestion methods which completely destroy the sample matrix and likely any particle-form information, resulting in a difference between particle analysis by FFF–ICP-MS and total silver analysis by digestion and ICP-MS being a result of the extraction procedures rather than the analytical techniques.

Please cite this article in press as: A.R. Poda, et al., J. Chromatogr. A (2011), doi:10.1016/j.chroma.2010.12.076

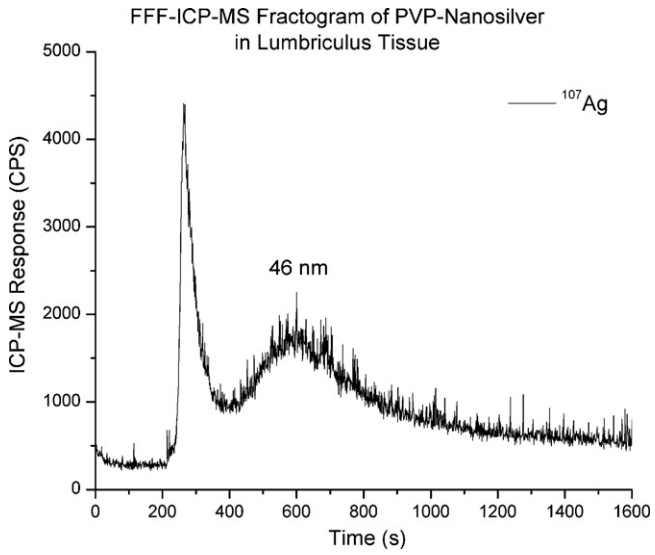

Fig. 7. FFF–ICP-MS fractogram of a PVP-coated silver nanoparticle extracted from *Lumbriculus* tissue by sonication in deionized water. FFF separation conditions were 1.0 mL/min channel flow and 0.75 mL/min cross flow with ICP-MS detection using ^{107}Ag.

4. Conclusions

FFF–ICP-MS provides a powerful tool for nanoparticle characterization, particularly metal or metal oxide particles, due to the sensitivity and selectivity of the ICP-MS detector. However, the particles must create a stable aqueous suspension for FFF analysis. The method has been shown to produce comparable results to other established sizing methods, such as DLS, for determination of particle hydrodynamic diameter. The results are also in qualitative agreement with primary particle sizes determined by microscopy. The FFF–ICP-MS technique is applicable to environmentally relevant particle concentrations and matrices, allowing detection and characterization of nanoparticles extracted from biological receptors after exposure. The ability to discern particle size and composition at μg/L concentrations further demonstrates the utility of the method for environmental applications.

Acknowledgments

The use of trade, product, or firm names in this report is for descriptive purposes only and does not imply endorsement by the U.S. Government. The tests described and the resulting data presented herein, unless otherwise noted, were obtained from research conducted under the Environmental Quality Technology Program of the United States Army Corps of Engineers by the USAERDC. Permission was granted by the Chief of Engineers to publish this information. The findings of this report are not to be construed as an official Department of the Army position unless so designated by other authorized documents. The authors also thank Frances Hill and Gail Blaustein of the USACE for their editorial comments.

References

[1] B. Karn, T. Kuiken, T.A. Otto, Environ. Health Perspect. 117 (2009) 1823.
[2] Y. Tian, B. Gao, C. Silvera-Batista, K.J. Ziegler, J. Nanopartic. Res. (2010), doi:10.1007/s11051-010-9912-7.
[3] M.R. Wiesner, G.V. Lowry, K.L. Jones, M.F. Hochella Jr., R.T. DiGiulio, E. Casman, E.S. Bernhardt, Environ. Sci. Technol. 43 (17) (2009) 6458.
[4] C.E. Mackay, M. Johns, J.H. Salatas, B. Bessinger, M. Perri, Integr. Environ. Assess. Manage. 2 (2006) 293.
[5] B. Nowack, Environ. Pollut. 150 (1) (2007) 5.
[6] N. Saleh, K. Sirk, Y.-Q. Liu, T. Phenrat, B. Dufour, K. Matyjaszewski, R.D. Tilton, G.V. Lowry, Environ. Eng. Sci. 24 (2007) 45.
[7] H.F. Lecoanet, J.-Y. Bottero, M.R. Wiesner, Environ. Sci. Technol. 38 (2004) 5164.
[8] D. Mavrocordatos, D. Perret, J. Microsc. 191 (1998) 83.
[9] G.G. Leppard, D. Mavrocordatos, D. Perret, Water Sci. Technol. 50 (2004) 1.
[10] W.A. Scrivens, J.M. Tour, K.E. Creek, L. Pirisi, J. Am. Chem. Soc. 116 (1994) 4517.
[11] Y. Song, V. Jimenez, C. McKinney, R. Donkers, R.W. Murray, Anal. Chem. 75 (2003) 5088.
[12] D.Y. Lyon, L.K. Adams, J.C. Falkner, P.J.J. Alvarez, Environ. Sci. Technol. 40 (2006) 4360.
[13] K.W. Powers, M. Palazuelos, B.M. Moudgil, S.M. Roberts, Nanotoxicology 1 (2006) 42.
[14] A. Akthakul, A. Hochbaum, F. Stellacci, A.M. Mayes, Adv. Mater. 17 (2005) 532.
[15] K.A. Howell, E.P. Achterberg, A.D. Tappin, P.J. Worsfold, Environ. Chem. 3 (2006) 199.
[16] J. Jamison, et al., Nanotechnology 20 (2009) 355702.
[17] C.J. Powell, J. Vac. Sci. Technol. A 8 (1980) 735.
[18] J.Y. Liu, J. Electron Microsc. 54 (2005) 251.
[19] A.R. Petosa, D.P. Jaisi, I.R. Quevedo, M. Elimelech, N. Turenkiji, Environ. Sci. Technol. 44 (2010) 6532.
[20] N.S. Wigginton, K.L. Haus, M.F. Hochella, J. Environ. Monit. 9 (2007) 1306.
[21] R.F. Domingos, M.A. Baalousha, Y. Ju-nam, M.M. Reid, N. Tufenkji, J.R. Lead, G.G. Leppard, K.J. Wilkinson, Environ. Sci. Technol. 43 (2009) 7277.
[22] J.R. Lead, K.J. Wilkinson, Environ. Chem. 3 (2006) 159.
[23] C.Y. Wang, et al., Meas. Sci. Technol. 18 (2007) 487.
[24] A. Bootz, V. Vogel, D. Schubert, J. Kreuter, Eur. J. Pharm. Biopharm. 57 (2004) 369.
[25] K. Tiede, A.B.A. Boxall, D. Tiede, S.P. Tear, H. David, J. Lewis, J. Anal. At. Spectrom. (2009), doi:10.1039/b822409a.
[26] M. Hassellov, J.W. Readman, J.F. Ranville, K. Tiede, Ecotoxicology 17 (2008) 344.
[27] J. Giddings, J. Chem. Phys. 49 (1968) 81.
[28] J. Giddings, K. Caldwell, Physical Methods of Chemistry, vol. IIIB, Wiley-Interscience, New York, 1989, pp. 120–139.
[29] M. Schimpf, Field-flow Fractionation Handbook, Wiley-Interscience, New York, 2000, pp. 71–79.
[30] S. Lee, P. Rao, S. Prabhakara, M.H. Moon, Anal. Chem. 68 (1996) 1545.
[31] S. Dubascoux, I. Le Hecho, M. Hassellov, F. Von Der Kammer, M. Potin Gautier, G. Lespes, J. Anal. At. Spectrom. 25 (2010) 613.
[32] U.S. Environmental Protection Agency, EPA/600/R-99/064, 2000, Office of Water, Washington, DC, 20460.
[33] J.F. Ranville, Environmental Effects of Nanoparticles and Nanomaterials, Clemson University, August 21–26, 2010 (Abstract).
[34] A.J. Bednar, A.R. Poda, A.J. Kennedy, A. Harmon, J.F. Ranville, D.M. Mitrano, J.A. Steevens, 31st Annual SETAC North America Meeting, Portland, OR, November 11, 2010.
[35] A.J. Kennedy, M.S. Hull, A.J. Bednar, J.D. Goss, J.A. Steevens, Environ. Sci. Technol. 44 (2010) 9571.